Simulation of nanosecond square pulse fiber laser based on nonlinear amplifying loop mirror

Guoliang Chen (陈国梁), Chun Gu (顾 春), Lixin Xu (许立新)*, Huan Zheng (郑 欢), and Hai Ming (明 海)

Department of Optics and Optical Engineering, University of Science and Technology of China, Hefei 230026, China

**Corresponding author: xulixin@ustc.edu.cn*

Received March 14, 2011; accepted April 14, 2011; posted online June 21, 2011

A nanosecond square pulse fiber laser based on the nonlinear amplifying loop mirror (NALM) is numerically analyzed by the nonlinear Schrödinger equation. The fiber cavity with a NALM has a tendency to provide pulse shaping effect with nonlinearity increasing in the NALM, and the nanosecond square pulse is generated by the pulse shaping effect. The numerical results show that the stable square pulse can be obtained when the parameters of the NALM are chosen appropriately. The generated square pulses have flat top and no internal structure.

OCIS codes: 140.3538, 060.2320, 060.3510, 140.4050.
doi: 10.3788/COL201109.091405.

Nanosecond square pulse laser has wide and important applications in many fields, such as optical communication, optical sensor, laser micromachining, and laser ablation[1,2]. In recent years, some new methods for nanosecond square pulse laser generation have been presented. Passively mode-locked fiber lasers through nonlinear polarization rotation (NPR), which can output nanosecond square pulses in 1 550-nm band, were demonstrated by Putnam *et al.* and output pulse with 10-ns pulse width and bandwidth of more than 60 nm was obtained[3]. In addition, Zhao *et al.* reported the generation of nanosecond square pulses in a passively mode-locked fiber ring laser made of purely normal dispersive long fibers[4]. These square pulse lasers are believed to be caused by the birefringence-related power clamping effect in the NPR cavity. Furthermore, the figure-eight mode-locking cavity with a nonlinear amplifying loop mirror (NALM) structure, which is widely used to generate ultrafast laser pulse from picoseconds to femtoseconds[5−7], has also been found to have the ability to generate nanosecond square pulse, which was observed for the first time by Richardson *et al.* in 1991[8]. In 2007, Schmieder *et al.* also reported the nanosecond square pulses from figure-eight cavity with NALM loops, with long highly nonlinear dispersion-shifted fiber[9]. However, these reports did not propose a mechanism explanation of the square pulse formation process.

In this letter, we numerically analyze the square pulse formation process in the figure-eight fiber cavity using the nonlinear Schrödinger equation. The numerical results show that the square pulse is caused by the pulse shaping effect of the NALM in the figure-eight cavity, and the influence of the fiber length in the NALM is also discussed.

Theoretically, this kind of nanosecond square pulse laser can operate at either 1.55-μm band or 1.06-μm band just by choosing different gain medium, erbium-doped fiber or ytterbium-doped fiber. The square pulse at 1.55 μm band can be used in fiber sensing and optic communications. Operating at 1.06 μm, we believe that the nanosecond square pulse can be amplified to high power and high pulse energy by using 1.06-μm high-power fiber amplifier, which will be useful in laser micromachining and laser ablation[10,11].

The setup of our square pulse laser system is shown in Fig. 1. It is constructed with a fiber amplifier, a section of the single-mode fiber (SMF), a polarization controller (PC), a 3-dB fiber coupler, an isolator, and an output coupler. The fiber loop on the right hand is known as the NALM, which is generally used as a nonlinear power switching or a saturable absorber device due to the self-phase modulation (SPM) effect in the fiber[12,13]. To introduce a sufficient nonlinear phase shift between the clockwise propagating light and the counterclockwise propagating light in the NALM, we use a segment of the SMF that is 300-m long between the PC and the fiber amplifier. The polarization management is implemented by the PC between the 3-dB coupler and the SMF. The fiber loop on the left is a unidirectional cavity. An isolator ensures unidirectional operation and that the pulse is exported from the output coupler.

This setup looks like the general figure-eight mode-locking fiber lasers, which can generate ultrashort pulse, because all of them are in the figure-eight architecture and utilize the NALM as the passive modulation device. However, in the general figure-eight mode-locking fiber laser, NALM is used as a saturable absorber without any power clamping effect. In our design, a segment of the 300-m SMF is used in the NALM, much longer than that of the general figure-eight mode-locking fiber lasers. The nanosecond square pulse generation depends on the pulse

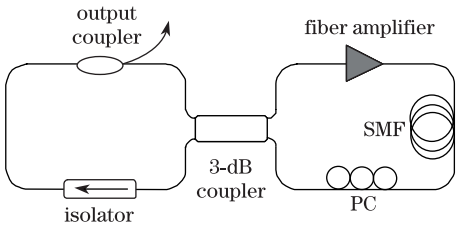

Fig. 1. Setup of the square pulse fiber laser.

reshaping effect and the power clamping effect of this specially designed NALM.

Square pulse generated in the figure-eight cavity with NALM can be simply explained with the power clamping effect of the NALM related to the nonlinear power transmission function, and this has been discussed in our previous report[12]. The figure-eight cavity can be considered as cascaded NALMs, and the transmittance of NALM is a function of the input power and the gain of the amplifier inside it. For a fixed gain in the NALM, a stable power region of the input power exists, where the output power of the cascaded NALM will come to a constant, while the power outside the region will be suppressed. For an initial weak pulse circling in a figure-eight cavity, after round trips in the cavity, the power in the stable power region is clamped to a steady power point, while the power outside the stable power region is gradually suppressed to zero. Thus, the square pulse is formed. Details of the square pulse shaping effect of the NALM can be referred in Ref. [14]. Even though this model can be used to explain the square pulse generation, they have several unrealistic assumptions, such as the single frequency, the amplifier with non-saturation, and the dispersion effect, which can also be ignored. Therefore, we propose a stricter theoretical model without these assumptions.

For a strict analysis, we numerically analyze the square pulse building process in the figure-eight fiber cavity using the nonlinear Schrödinger equation, and some other effects such as dispersion and gain saturation are also considered. Compared with the nonlinear transmission function method, the results of this analysis are believed to be much more suitable to the real situation. In our analyses, the polarization and the birefringence effect are neglected because the numerical result is independent of them; the model can also be simplified. The theoretical model in our numerical analyses can be seen in Fig. 2, where the PC is neglected. The isolator in the left ring also not considered because the unidirectional propagation is easily implemented by the computational procedure. At the beginning, we assume that an initial Gaussian pulse from the fluctuation, weak and wide, has appeared in the cavity. The envelope of the complex amplitude of the initial Gaussian pulse can be expressed as

$$A = \sqrt{P_0}\exp(-T^2/2T_0^2), \tag{1}$$

where T_0 is the half width (at $1/e$ intensity point) of the pulse and P_0 is the pulse peak power.

The simulation started at the 3-dB coupler. The evolution of this initial pulse in the figure-eight cavity we design is then studied. Passing the 3-dB coupler, the pulse is divided into two parts. The optical fields in the straight arm and the cross arm are denoted as U and V, respectively, which can be written as[13]

$$U = \sqrt{\rho}A, \quad V = \mathrm{i}\sqrt{1-\rho}A, \tag{2}$$

where ρ is the power coupling ratio of the fiber coupler; here we set $\rho = 0.5$.

Considering the group velocity dispersion (GVD), SPM, attenuation, and the gain bandwidth, optical pulse propagating in the fiber cavity can be described by the nonlinear Schrödinger equation[16] as in which A can be replaced by U, V, or A',

$$\frac{\partial A}{\partial z} + \frac{\mathrm{i}}{2}\beta_2\frac{\partial^2 A}{\partial T^2} - \frac{1}{2}g\frac{1}{\Delta\omega^2}\frac{\partial^2 A}{\partial T^2} = \mathrm{i}\gamma|A|^2 A + \frac{1}{2}(g-\alpha)A, \tag{3}$$

where β_2 is the GVD parameter, γ is the nonlinear coefficient, $\Delta\omega$ is the gain bandwidth of the fiber amplifier, g is the gain coefficient, and $g = 0$ for the undoped fiber. For the doped fiber, the gain coefficient can be expressed as

$$g = g_0 \cdot \exp\left(-\frac{\int |A|^2\,\mathrm{d}t}{E_\mathrm{s}}\right), \tag{4}$$

where g_0 is the gain coefficient of the small signal and E_s is the saturated energy.

The parameters' values used in our simulation are shown in Table 1. After traveling one round in the right loop and recombined at the coupler, the optical field at the output port of the NALM is given by $A' = \sqrt{\rho}U' + \mathrm{i}\sqrt{1-\rho}V'$. Subsequently, the pulse propagates in the unidirectional fiber ring on the left and enters the NALM again to begin the next trip after an export loss at the coupler.

In the simulation, the initial pulse width and the peak power are set to $T_0 = 30$ ns and $P_0 = 25$ W, respectively, and the output loss is set to 5%. Equation (3) is numerically solved in the split-step Fourier method. The simulation results can be seen in Fig. 3. In the beginning several loops, both the pulse rising and falling edges are suppressed rapidly while the pulse center is amplified. The pulse profile is shaped gradually close to a square waveform and has no internal structure. This can be attributed to the shaping effect of the NALM with the 300-m-long fiber. After about 10 rounds, the pulse becomes stable and is kept in square shape.

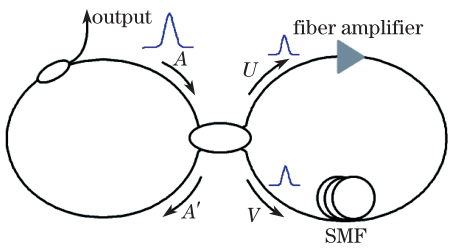

Fig. 2. Simplified theoretical model in our numerical analyses.

Table 1. Parameters Used in the Simulation of the Square Pulse Generation

Parameter	Value
β_2 ($\mathrm{ps^2\cdot km^{-1}}$)	22
γ ($\mathrm{W^{-1}\cdot km^{-1}}$)	3
g_0 ($\mathrm{dB\cdot km^{-1}}$)	223
$\Delta\omega$ (THz)	10
α ($\mathrm{dB\cdot km^{-1}}$)	0.02
L_1 (m)	300
L_2 (m)	1
E_s (μJ)	50

α is the attenuation of the fiber, L_1 is the length of the SMF in the NALM, and L_2 stands for the length of the rare-earth-doped fiber in the fiber amplifier.

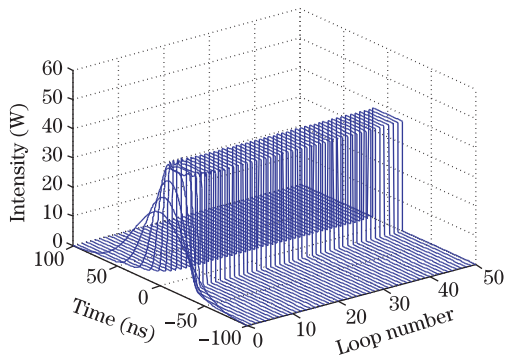

Fig. 3. Simulation result of the formation of the square pulse in a figure-eight fiber laser cavity with a section of 300-m SMF in the NALM.

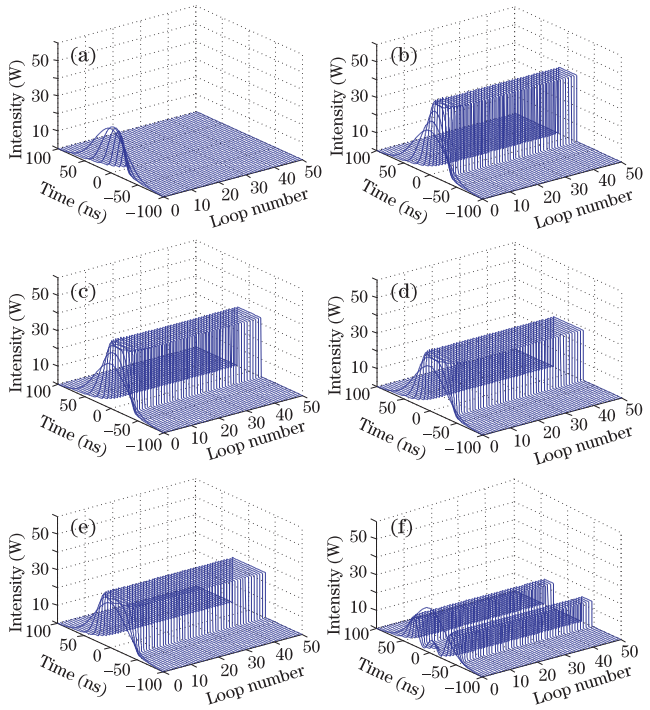

Fig. 4. Formations of square pulse with the NALM in different lengths. The fiber length L_1 is (a) 250, (b) 300, (c) 350, (d) 400, (e) 450, and (f) 800 m, respectively.

For a further comparison among the formations of square pulse with the NALM in different lengths, we set L_1 to 250, 300, 350, 400, 450, and 800 m successively and keep other parameters unchanged. The results are shown in Fig. 4. We can find that, with a fixed gain in the amplifier, the square pulse can be generated if L_1 is chosen in an adequate region. When L_1 is set to 250 m, the pulse dissipates quickly, as shown in Fig. 4(a). If L_1 is chosen appropriately, such as Figs. 4(b)–(e), the square pulses are generated and get into a stable operation. In this region of L_1, the longer the NALM that is chosen, the wider will be the square pulse obtained. However, if we continue to increase the length of the fiber in the NALM, for instance to 800 m, we will get a multi-square pulse operation, as shown in Fig. 4(f). Hence, we can conclude that in the square pulse fiber laser, L_1 is very important and thus must be chosen appropriately.

Additionally, using the same method, we also calculated the operation of a shorter figure-eight cavity consisting of only 20-m-long SMF in the NALM, which is the standard length of the NALM in the general mode-locking fiber laser. By appropriately setting the small signal gain and the saturable energy, stable ultrashort pulse can be generated from a weak signal. In this case, the pulse shape obtained is approximate to a hyperbolic secant function profile, which is clearly different from the square pulse mentioned above. Because with a SMF of much shorter length, such as 20 m, the power switching threshold of the NALM increases to a much higher level. With the same pump power level, the NALM only works as a general saturable absorber without any power clamping effect to generate square pulse, and the pulse width in the cavity is only compressed by the NALM repeatedly. Finally, the pulse will be kept stable in a Gaussian or a hyperbolic secant-like shape, with a time duration dominated by the dispersion map of the fiber cavity. This is also in accordance with many experiments involving the general figure-eight mode-locking fiber laser[7].

In conclusion, we numerically analyze a nanosecond square pulse laser source based on the figure-eight fiber cavity with a special NALM structure, which has hundreds of meters SMF. We numerically prove that the stable square pulse without internal structure can be generated if the length of the NALM is sufficient. The square pulse generation is based on the pulse shaping effect of the NALM, and the pulse width depends critically on the length of the NALM. We find that under the same pump power, wider square pulse can be obtained if we choose a longer NALM before the multi-square pulse appears. We believe that this square pulse fiber laser is a special kind of mode-locking fiber laser and will have wide potential applications.

References

1. X. Peng, B. Jordens, A. Hooper, B. W. Baird, W. Ren, L. Xu, and L. Sun, Proc. SPIE **7193,** 719324 (2009).
2. C. Liu, X. L. Mao, S. S. Mao, X. Zeng, R. Greif, and R. E. Russo, Anal. Chem. **76,** 379 (2004).
3. M. A. Putnam, M. L. Dennis, I. N. Duling III, C. G. Askins, and E. J. Friebele, Opt. Lett. **23,** 138 (1998).
4. L. M. Zhao, D. Y. Tang, T. H. Cheng, and C. Lu, Opt. Commun. **272,** 431 (2006).
5. Y. Zhao, S. Min, H. Wang, and S. Fleming, Opt. Express **14,** 10475 (2006).
6. J. W. Nicholson, S. Ramachandran, and S. Ghalmi, Opt. Express **15,** 6623 (2007).
7. IrI N. Duling III, Opt. Lett. **16,** 539 (1991).
8. D. I. Richardson, R. I. Laming, D. N. Payne, V. Matsas, and M. W. Phillips, Elect. Lett. **27,** 542 (1991).
9. D. Schmieder, P. L. Swart, and A. Booysen, in *Proceedings of AFRICON 2007* 4401621 (2007).
10. B. Zhao, K. Duan, W. Zhao, C. Li, and Y. Wang, Chin. Opt. Lett. **8,** 404 (2010).
11. Z. Yang, X. Hu, Y. Wang, W. Zhang, and W. Zhao, Chin. Opt. Lett. **9,** 041401 (2011).
12. M. E. Fermann, A. Haberl, M. Hofer, and H. Hochreiter, Opt. Lett. **15,** 752 (1990).
13. N. J. Doran and David Wood, Opt. Lett. **13,** 56 (1988).
14. H. Zheng, L. X. Xu, A. T. Wang, C. Lu, and H. Ming, Proc. SPIE **7276,** 72761F (2008).
15. G. P. Agrawal, Phys. Rev. A. **44,** 7493 (1991).